

**Impact of
supersaturation**

A. Gettelman and
D. E. Kinnison

The global impact of supersaturation in a coupled chemistry-climate model

A. Gettelman and D. E. Kinnison

National Center for Atmospheric Research, Boulder, CO, USA

Received: 3 November 2006 – Accepted: 22 November 2006 – Published: 1 December 2006

Correspondence to: A. Gettelman (andrew@ucar.edu)

Title Page

Abstract

Introduction

Conclusions

References

Tables

Figures

◀

▶

◀

▶

Back

Close

Full Screen / Esc

Printer-friendly Version

Interactive Discussion

Abstract

Ice supersaturation is important for understanding condensation in the upper troposphere. Most general circulation models however do not permit supersaturation. In this study, a coupled chemistry climate model, the Whole Atmosphere Community Climate Model (WACCM), is modified to include supersaturation for the ice phase. The study is intended as a sensitivity experiment, to understand the potential impact of supersaturation, and of expected changes to stratospheric water vapor, on climate and chemistry. Results indicate that high clouds decrease and water vapor in the stratosphere increases nearly linearly with supersaturation (20% supersaturation increases water vapor by nearly 20%). The stratospheric Brewer-Dobson circulation slows at high southern latitudes, consistent with slight changes in temperature likely induced by changes to cloud radiative forcing. The cloud changes also cause an increase in the seasonal cycle of near tropopause temperatures, increasing them in boreal summer over boreal winter. There are also impacts on chemistry, with small increases in ozone in the tropical lower stratosphere driven by enhanced production. The radiative impact of changing water vapor is dominated by the reduction in cloud forcing associated with fewer clouds ($\sim+0.6 \text{ Wm}^{-2}$) with a small component likely from radiative effect (greenhouse trapping) of the extra water vapor ($\sim+0.2 \text{ Wm}^{-2}$), consistent with previous work. Representing supersaturation is thus important, and changes to supersaturation resulting from changes in aerosol loading for example, might have a modest impact on global radiative forcing, mostly through changes to clouds. We do not see evidence of a strong impact of water vapor on tropical tropopause temperatures.

1 Introduction

Condensation in the atmosphere occurs when the vapor pressure of water or ice is higher than the saturation vapor pressure over liquid or ice (Murphy and Koop, 2005). While this statement is basically correct for liquid, where supersaturations of more than

ACPD

6, 12433–12468, 2006

Impact of supersaturation

A. Gettelman and
D. E. Kinnison

Title Page

Abstract

Introduction

Conclusions

References

Tables

Figures

◀

▶

◀

▶

Back

Close

Full Screen / Esc

Printer-friendly Version

Interactive Discussion

EGU

Impact of supersaturationA. Gettelman and
D. E. Kinnison

Title Page

Abstract

Introduction

Conclusions

References

Tables

Figures

◀

▶

◀

▶

Back

Close

Full Screen / Esc

Printer-friendly Version

Interactive Discussion

a fraction of a percent rarely persist, it is not true for ice processes (Kärcher and Haag, 2004). Significant supersaturations over ice are seen routinely in the atmosphere from aircraft (Jensen et al., 2005), balloons and radiosondes (Spichtinger et al., 2003a) and satellites (Jensen et al., 1999; Spichtinger et al., 2003b; Gettelman et al., 2006).

5 This is not surprising when one considers the condensation and freezing process for molecules of H₂O in the atmosphere. Freezing is essentially a 2 step process, requiring condensation and then freezing (Koop et al., 2000). Since the saturation vapor pressure over water is higher than that over ice at low temperatures, we might then see large ice supersaturations before freezing occurs.

10 Supersaturation may have significant impacts on the state of the atmosphere. Making the most simple assumptions, if one allows 20% more water to be present before condensation, and stratospheric water vapor is limited by temperature dependent condensation at the tropical tropopause (Holton and Gettelman, 2001), we might expect a corresponding increase of 20% in upper tropospheric and stratospheric water vapor, and a drop in high cloud cover. Changes to the condensation threshold would be due to differences in water activity (Koop et al., 2000) which might arise due to variations in the population of aerosols for example.

Such changes would have significant impacts on climate and chemistry. Changes in high cloud cover would have significant effects on tropospheric climate and the radiation balance of the atmosphere. A reduction in high clouds may substantially increase outgoing longwave radiation at the top of the atmosphere, leading to a cooling effect on the climate system. Alternatively, since the overall effect of clouds is to cool (Cess, 2005) a reduction in clouds might warm the planet.

25 Changes in stratospheric water may have effects on both chemistry and climate. Since water is the dominant species in the stratospheric hydrogen budget, we might also expect differences in hydrogen radicals (HO_x = OH + HO₂) in the stratosphere, leading to changes in ozone and other trace species chemistry, particularly where hydrogen radicals dominate ozone chemistry in the lower stratosphere (Wennberg et al., 1994). In addition, stratospheric water vapor changes have been shown to

impact tropospheric temperatures (Forster and Shine, 2002). Recently Stuber et al. (2001) and others (Stuber et al., 2005; Joshi et al., 2003) have speculated about a “stratospheric water vapor feedback” whereby changes in greenhouse gases force increases in tropopause temperatures, and these temperature changes induce increases in stratospheric water which may further increase tropospheric temperatures.

Most global models, however, use large-scale closure schemes for condensation that include assumptions that do not permit supersaturation with respect to liquid or ice (for example, Rasch and Kristjansson, 1998). For very large (100s of km) regions represented by global model grid cells this was thought to be a reasonable assumption. However, recent work with aircraft data (Gierens and Spichtinger, 2000) on long flight tracks and with satellites (Gettelman et al., 2006) has shown that even at these scales supersaturation may be present.

To better understand potential aerosol indirect effects on climate, more detailed treatments of ice cloud nucleation and microphysics are being developed for global models. Including representations of supersaturation will be critical for appropriately nucleating ice clouds (Kärcher et al., 2006) and for representing the affects of aerosol nucleation and freezing for ice clouds (Kärcher and Lohmann, 2002a,b).

Thus representation of supersaturation in global models is critically important for understanding both stratospheric chemistry and tropospheric climate. In this work we present simple modifications to a coupled chemistry climate model which permit bulk supersaturation with respect to ice, and use the model to understand the impact of supersaturation on simulated climate and chemistry of the upper troposphere and lower stratosphere (UT/LS) region. This is not necessarily the ideal treatment of supersaturation, but within the context of a coupled chemistry climate model it allows us to examine the impact of supersaturation and increased stratospheric water vapor in a geophysical way and understand feedbacks on stratospheric chemistry and atmospheric dynamics.

The model and methodology is described in Sect. 2, the results are presented in Sect. refsec:results and conclusions are contained in Sect. 4.

Impact of supersaturationA. Gettelman and
D. E. Kinnison

Title Page

Abstract

Introduction

Conclusions

References

Tables

Figures

◀

▶

◀

▶

Back

Close

Full Screen / Esc

Printer-friendly Version

Interactive Discussion

2 Methodology

The principle behind this work is to take a state of the art coupled chemistry climate model, and allow grid box averaged supersaturation in the simulations. Below we describe the model, the simple changes we have made, and the simulations we have performed. The purpose is not so much to evaluate the performance of the simulations against observations but to examine the differences as a result of supersaturation.

2.1 Model description

For this work we have utilized the Whole Atmosphere Community Climate Model, Version 3 (WACCM3) developed at the National Center for Atmospheric Research (NCAR). WACCM3 is a state of the art coupled chemistry climate model that spans the atmosphere from the surface to the lower thermosphere (~ 140 km). The model is described by Garcia et al. (2006)¹, and performs well relative to observations and to other coupled models (Eyring et al., 2006). We note some of the relevant features for this study below.

WACCM3 is based on the framework of the Community Atmosphere Model, version 3 (CAM3), a General Circulation Model (GCM), described by Collins et al. (2006). WACCM3 uses CAM3 as its base, and adds parameterizations for chemistry and upper atmospheric processes. The CAM model top is typically 2 hPa (45 km), while the WACCM model top is 5×10^{-6} hPa (140 km). The chemistry module for WACCM3 is derived from the three dimensional chemical transport Model for Ozone and Related chemical Tracers (MOZART) (Brasseur et al., 1998; Horowitz et al., 2003; Kinnison et al., 2006²). The chemistry package comprises 56-species representing chemical and

¹Garcia, R. R., Marsh, D., Kinnison, D., Boville, B. A., and Sassi, F.: Simulations of secular trends in the middle atmosphere, 1950–2003, J. Geophys. Res., submitted, 2006.

²Kinnison, D. E., Brasseur, G. P., Walters, S., et al.: Sensitivity of Chemical Tracers to Meteorological Parameters in the MOZART-3 Chemical Transport Model, J. Geophys. Res., submitted, 2006.

Impact of supersaturation

A. Gettelman and
D. E. Kinnison

Title Page

Abstract

Introduction

Conclusions

References

Tables

Figures

◀

▶

◀

▶

Back

Close

Full Screen / Esc

Printer-friendly Version

Interactive Discussion

**Impact of
supersaturation**A. Gettelman and
D. E. Kinnison

Title Page

Abstract

Introduction

Conclusions

References

Tables

Figures

◀

▶

◀

▶

Back

Close

Full Screen / Esc

Printer-friendly Version

Interactive Discussion

physical processes in the middle atmosphere, including inorganic nitrogen, hydrogen, chlorine and bromine chemistry, along with CH₄ and its degradation products. Heterogeneous processes on sulfate aerosols and polar stratospheric clouds are included. Surface fluxes of chemical species as well as NO_x (NO+NO₂) and CO sources from lightning and aircraft emissions are included, as are wet and dry deposition. The chemistry is coupled in-line to the model dynamics and radiation, so that chemical species (such as ozone) affect model heating rates.

WACCM3 uses CAM3 routines for condensation and the hydrologic cycle. The model has a bulk microphysics scheme with prognostic vapor, liquid and ice that are conserved and advected (Rasch and Kristjansson, 1998). Fractional cloudiness is the trigger for condensation and it is constrained by relative humidity (RH) following Slingo (1987), such that condensation begins at 90% relative humidity. CAM uses a “combined” relative humidity that reflects relative humidity with respect to water for temperatures above −10°C, with respect to ice below −30°C, and a linear combination of the saturation vapor pressure between these limits. The simulation of the hydrologic cycle is described by Boville et al. (2006).

2.2 Supersaturation

Because the bulk microphysics formulation of Rasch and Kristjansson (1998) used in WACCM3 does not permit supersaturation with respect to ice, we have modified the formulation of the Slingo (1987) cloud fraction scheme so that the critical relative humidity threshold for starting to form cloud increases when ice is present, and can be higher than 100% RH. In the standard WACCM3 case, cloud begins to form at a relative humidity of 90%, and 100% cloud cover occurs at 100% RH. This has been modified for ice clouds so that cloud does not begin to form until RH=100% and full (100%) cloud cover occurs at RH=120%. These values are the model “merged” relative humidity. As noted above, this means that for temperatures below −30°C, condensation will not fully occur until RH=120% over ice.

This is of course not the ideal or preferable way to represent supersaturation in a

model. Other approaches, such as the treatment of [Kärcher and Lohmann \(2002a\)](#), allow proper representation of condensation of ice through homogeneous and/or heterogeneous nucleation and freezing of cloud particles on to aerosols. However, the bulk representation described above is internally consistent with the WACCM3 hydrologic cycle, and we hypothesize that this will increase the amount of water vapor and decrease condensation and clouds in the simulation in a geophysically realistic way. Other model simulations which have attempted to investigate the effect of increases in stratospheric water vapor have generally fixed water or explicitly enhanced its concentration (e.g. [Forster and Shine, 2002](#), [Stuber et al., 2005](#) and [Stenke and Grewe, 2005](#)).

2.3 Simulations

For analysis, two 22 year integrations of WACCM3 were performed at $4^\circ \times 5^\circ$ horizontal resolution. The model has 66 levels in the vertical with resolution of about 1km in the UT/LS region. In one (Base) simulation the standard WACCM3 configuration was used with annually repeating 1995 boundary conditions. This includes Sea Surface Temperatures from 1995 and levels of CO_2 and chlorine compounds appropriate for that year. An identical “supersaturated” (SSAT) simulation was run with the same boundary conditions, but with the code modified to allow supersaturation for the ice phase as described above. The last 15 years of model output is used for all analyzes. We have repeated the analyzes in this paper on varying sets of 5 and 10 year periods from each one. All the conclusions are qualitatively robust relative to inter-annual variations. There are some quantitative differences in the extra-tropics where variability is larger, but the conclusions are unchanged.

Impact of supersaturation

A. Gettelman and
D. E. Kinnison

Title Page

Abstract

Introduction

Conclusions

References

Tables

Figures

◀

▶

◀

▶

Back

Close

Full Screen / Esc

Printer-friendly Version

Interactive Discussion

3 Results

In this section we discuss the main results from comparing the two WACCM3 simulations, referred to as the “Base” and “SSAT” (or “supersaturated”) cases. We will first discuss cloud and water vapor fields since these are most directly impacted by the changes. We will then discuss the impact on the circulation (transport) and temperature, including chemical tracers of transport. We will then discuss ozone and other chemical species, and finally examine the radiative balance of the simulations and how they are related to other differences.

3.1 Clouds

In the tropics, the maximum zonal mean cloud fraction for high clouds in the base simulation is found at 200–250 hPa (0.4). At the tropopause, cloud fraction is 0.2. The latter is almost exclusively cirrus clouds generated from the stratiform cloud parameterization. By raising the threshold for high (ice) cloud formation, the mean cloud fraction is decreased by nearly 50% (absolute, cloud fraction goes down by 0.17), as indicated in Fig. 1a. At pressures above 600 hPa the differences are minor. The largest decreases are at 200 hPa and coincident with the maximum high level cloudiness. There are smaller changes at high latitudes. Analysis of cloud changes sorted by optical depth indicates that most of the changes are to high clouds with optical depth less than 3 (cirrus clouds). Regionally the largest changes occur where the cloud fractions are highest, in the tropical Western Pacific region. Changes are larger in June–August than in December–February.

Consistent with the change in cloudiness, cloud ice mixing ratio goes down almost everywhere in the simulations with supersaturation (Fig. 1b). In the tropical upper troposphere, the change is up to –50% and maximizes near the freezing level. Cloud liquid is less affected. As a result total precipitable water decreases by only 10% in tropics (not shown).

Associated with this decrease in cloudiness however is a small global increase in

Impact of supersaturation

A. Gettelman and
D. E. Kinnison

Title Page

Abstract

Introduction

Conclusions

References

Tables

Figures

◀

▶

◀

▶

Back

Close

Full Screen / Esc

Printer-friendly Version

Interactive Discussion

global mean precipitation. The global increase in both rate and total is about 4%, and occurs mostly in the central to eastern Pacific Inter-Tropical Convergence Zone (ITCZ), and over the Atlantic ocean. There are slight decreases in precipitation over the Indian Ocean. It is likely that the delay of condensation is causing precipitation to occur at a higher rate, though it is not clear why this would affect total precipitation, except if the changes were to actually change the lifetime of humidity in the troposphere. The base simulation generally has too much precipitation in the central to eastern Pacific and the Indian ocean.

The radiative impact of clouds is usually assessed by examining the cloud forcing, which is the difference of the top of atmosphere radiation and the radiation assuming a clear sky (e.g. Ramanathan et al., 1989). Short and longwave cloud forcing are calculated from the model using this method. With supersaturation and a reduction in cloudiness, the magnitudes of both shortwave and longwave forcing drop. The global average longwave cloud forcing is 30 Wm^{-2} in the base case, and drops by 7 Wm^{-2} . The shortwave cloud forcing is -53 Wm^{-2} (clouds cool in the shortwave), and drops by -8 Wm^{-2} (to -45 Wm^{-2}) The net cloud forcing in the model is -22 Wm^{-2} and changes by $+0.6 \text{ Wm}^{-2}$. We expect reductions in longwave forcing with the reduction in cirrus clouds, but the magnitude of the reductions is large enough to strongly reduce shortwave cloud forcing as well (and slightly more than the total longwave forcing), particularly over the Indian Ocean. The cloud forcing changes appear largely due to changes in simulated cirrus clouds. Changes in clouds are slightly larger during June–August than during December–February.

3.2 Water vapor

Like the changes in cloudiness, the changes in water vapor are expected from the changes to the physics in the simulation. In general, with the reduction in condensation, specific humidity and relative humidity (RH) increase in the upper troposphere throughout the stratosphere. This is illustrated in Fig. 2. Where RH is highest in the tropical UT/LS region and at high polar latitudes, RH increases by up to 12–15% (Fig. 2a).

Impact of supersaturation

A. Gettelman and
D. E. Kinnison

Title Page

Abstract

Introduction

Conclusions

References

Tables

Figures

◀

▶

◀

▶

Back

Close

Full Screen / Esc

Printer-friendly Version

Interactive Discussion

Impact of supersaturationA. Gettelman and
D. E. Kinnison

Title Page

Abstract

Introduction

Conclusions

References

Tables

Figures

◀

▶

◀

▶

Back

Close

Full Screen / Esc

Printer-friendly Version

Interactive Discussion

There are slight decreases in humidity at lower altitudes, below 300 hPa in the tropical middle troposphere, which is very close to the average freezing level in the simulations. This is perhaps due to raising of the condensation level. Water vapor (specific humidity) increases as well in the regions where the large scale cloudiness scheme controls its value: mostly in the tropical tropopause layer (Fig. 2b). Note that RH increases in the stratosphere as well, but the values are insignificant. Water vapor increases of up to 20% are seen just above the tropical tropopause, with values increasing everywhere in the stratosphere, but by lower percentage amounts as air is further from the tropical tropopause and RH is only a few percent.

Understanding the seasonality of these changes is critical for understanding their cause. Water vapor values in the tropical lower stratosphere have a strong seasonal cycle (Mote et al., 1996) with a minimum in boreal winter and a maximum in boreal summer. This signal propagates vertically from the tropical tropopause as the air ascends due to the Brewer-Dobson circulation (Holton et al., 1995). The simulated “tropical tape recorder” signal (Mote et al., 1996) in water vapor from the base run is illustrated in the top panel of Fig. 3. Figure 3 shows a composite repeated annual cycle based on monthly means of the base simulation.

In general the annual cycle in the base WACCM3 simulation (top panel of Fig. 3) compares quite well to observations of water vapor in the stratosphere (Randel et al., 2001; SPARC, 2000). The minimum in water vapor occurs 1–2 months later than observations in the simulation, but the speed of propagation and attenuation is appropriate. Mixing ratios in the base case are generally 0.5 ppmv dry relative to observations, slightly more dry in boreal summer. For a full discussion of WACCM3 performance in this regard, see Garcia et al. (2006)¹.

The lower panel of Fig. 3 illustrates the differences between the model with supersaturation and the base case. Consistent with Fig. 2, water vapor increases almost everywhere, except in the troposphere below 100 hPa from January–March.

The increases are largest in boreal summer and fall from September–November. This is the period when cooling of the tropical tropopause region is strongly affecting

water vapor. Note that the differences between the simulations occur in the lower stratosphere and also propagate vertically. Overall there is nearly 1 part per million by volume (ppmv) more water vapor in the stratosphere in the supersaturation case. Overall the changes improve the simulation of water vapor in the stratosphere. In order to determine the cause of these changes, it is instructive to examine changes in temperature as well.

3.3 Temperature

Figure 4 illustrates the annual zonal mean change in temperature between the simulations. There are slight and coherent changes in temperature in the simulations with supersaturation. In general there are decreases of annual mean temperature in the upper tropical troposphere by 0.5–1°K. These changes may be due to several factors. First, the increase in water vapor in the upper troposphere will increase clear sky cooling. Second, the decrease in cloud fraction decreases any heating due to local absorption by clouds and increases the effect of the clear sky cooling. The region of cooling in the tropical upper troposphere (400–100 hPa) in Fig. 4 is similar to the region of reduced cloudiness in Fig. 1a. In the lower stratosphere there is an increase in temperature of up to 1.5°K. This is consistent with decreased clouds below this region leading to more longwave absorption in the lower stratosphere. It may also indicate changes in the strength of the stratospheric wave-driven Brewer-Dobson circulation, which will be discussed in more detail below. Consistent with a change in the global circulation, there are colder temperatures in the southern polar stratosphere. At 85 hPa, the spatial pattern of tropical temperature changes has increases nearly everywhere along the equator, with maximum changes over the equatorial eastern Pacific, and the equatorial western Pacific. In the upper stratosphere and mesosphere, there is cooling of up to 1.5 K (not shown), consistent with increased water vapor throughout the stratosphere below.

The temperature changes are not symmetric throughout the year. Figure 5 is similar to Fig. 3 but illustrates the equatorial temperature distribution up to 1hPa. Temperatures

Impact of supersaturation

A. Gettelman and
D. E. Kinnison

Title Page

Abstract

Introduction

Conclusions

References

Tables

Figures

◀

▶

◀

▶

Back

Close

Full Screen / Esc

Printer-friendly Version

Interactive Discussion

**Impact of
supersaturation**A. Gettelman and
D. E. Kinnison

Title Page

Abstract

Introduction

Conclusions

References

Tables

Figures

◀

▶

◀

▶

Back

Close

Full Screen / Esc

Printer-friendly Version

Interactive Discussion

decrease slightly where water vapor in Fig. 3 decreases, and the largest temperature increases near the tropopause in Fig. 5b are coincident with the largest water vapor increases at this level (Fig. 3b). Thus it appears that temperature changes are affecting the annual cycle in water vapor differences between the simulations. There are still increases in stratospheric water vapor everywhere in the supersaturation simulation. Consistent with Fig. 5b, tropical cold point tropopause temperature in the supersaturation simulation warms by 1°K in boreal summer, with virtually no change in boreal winter. High latitude changes in temperature in the southern polar stratosphere are also largest in September–November (not shown).

Thus, the amplitude of the annual cycle of temperature around the tropical tropopause increases in the supersaturation case, with larger temperature changes in July–October than in December–March. This appears to be due to larger changes (reductions) in tropical high clouds in boreal summer, with the result that there is an extra 5–15 Wm⁻² of outgoing longwave radiation in this season, which is the likely cause of the warm temperatures. Seasonal changes to the residual circulation in the stratosphere may also play a role.

3.4 Circulation and long lived trace species

Given the decreases in temperature seen at high latitudes in Fig. 4 and the increases in temperature in the tropics, it is obvious to ask if circulation changes might account for this difference. A decrease in the equatorial upwelling and corresponding decrease in high latitude descent would alter temperatures in a similar manner to Fig. 4, increasing temperatures in the tropics (reduced adiabatic cooling) and decreasing them at high latitudes (decreased adiabatic warming). To better understand the stratospheric circulation, we have calculated the Transformed Eulerian Mean (TEM) circulation (Andrews et al., 1987) for both runs. The annual residual mean vertical motion (\bar{w}^*) for the base case is plotted in Fig. 6a, and features upward motion in the tropics and downward motion at the poles.

Figure 6b illustrates the percent difference between the supersaturation and base

simulations. Relative to the base case, down-welling at high latitudes of the southern hemisphere in the supersaturation run is 20% lower. In addition, there is a reduction of the meridional gradient of the circulation in the middle stratosphere: increases on the edges of the down-welling regions mean less (negative) down-welling, and decreases on the edges of the upwelling indicate less (positive) upwelling. These changes are small however in absolute terms. There are slightly larger changes at higher altitudes (lower pressures) near 1 hPa. This is near the region where temperatures are cooling (Fig. 4).

Figure 7 illustrates the annual cycle of the TEM meridional velocity, \bar{v}^* , in Fig. 7a, and the annual cycle of the TEM vertical velocity, \bar{w}^* , in Fig. 7b, at 61 hPa, near the maximum difference in tropical temperatures. In the tropics from May to September there are slight decreases in tropical upwelling (Fig. 7b), which are consistent with the temperature changes in Fig. 4. In addition, there are decreases in downward vertical velocity at high southern latitudes in Fig. 7b. These changes are also consistent with changes to the vertical velocity. The horizontal velocity (Fig. 7a), shows a decrease in southward meridional flow in the supersaturation case throughout most of the year, and especially from July–October. These differences are associated with an increase in the speed of the southern hemisphere polar jet in the simulations.

Another way of checking for consistency of the vertical motion changes is to examine long lived tracers. Figure 8 plots the percent change in concentration (mixing ratio) of CH₄ (Fig. 8a) and the temporal change in the Age of Air (Fig. 8b). Methane has a tropospheric source and decay in the stratosphere. Figure 8a indicates decreases at southern polar latitudes, consistent with a slowing of the stratospheric circulation and (more time for chemical destruction). It does not appear as if there are changes in HO_x to cause chemical changes in methane (see discussion of chemistry below).

A similar picture is also seen by calculating the Age of Air (Waugh and Hall, 2002) in the stratosphere from the simulations (Fig. 8b). Southern polar latitudes have an older age in the supersaturation simulation by 2–6 months (with a mean age of 4–4.5 years). This is consistent with the circulation and chemistry changes, indicating a slowing of

Impact of supersaturationA. Gettelman and
D. E. Kinnison

Title Page

Abstract

Introduction

Conclusions

References

Tables

Figures

◀

▶

◀

▶

Back

Close

Full Screen / Esc

Printer-friendly Version

Interactive Discussion

the stratospheric circulation, with a change occurring mostly in Southern Hemisphere winter.

The simulations have also been examined for significant changes to the tropospheric circulation. In general there appear to be small changes in the northern hemisphere tropospheric circulation. The increase in the southern hemisphere stratospheric polar jet appears to extend all the way to the surface (but changes are only of the order of 1–3 ms⁻¹). There is virtually no change in the 200 hPa streamfunction.

3.5 Ozone and other species

The changes in temperature (Fig. 4) and water vapor (Fig. 2) due to allowing supersaturation will also likely have impacts on chemistry in the UT/LS region and throughout the stratosphere. One of the benefits of using WACCM3 is that changes to chemical species as a result of the changes to physics can be assessed in a consistent, coupled framework. One of the difficulties of using a coupled chemistry-climate model is that discerning causes in the coupled system is difficult (as will be shown below).

Figure 9 plots the annual zonal mean percent difference in ozone between the two simulations. O₃ increases in the tropical lower stratosphere by 5–10% in the supersaturation simulation. It decreases slightly in the middle troposphere, as well as decreasing by up to 18% in the southern hemisphere lowermost stratosphere.

The seasonal cycle of tropical ozone changes is illustrated in Fig. 10. The changes (in ppbv) in Fig. 10a need to be taken in the context of ozone concentrations, so that the middle stratospheric changes of ±200 ppbv are in percentage terms (Fig. 10b) smaller than the 50 ppbv change in the lower stratosphere. In the lower stratosphere, the ozone increase maximizes in July to October, and is consistent with the seasonal cycle of temperature (Fig. 5) and water vapor (Fig. 3) changes. This change in ozone is also consistent with slowing of the stratospheric circulation, which would allow more time for ozone production in the tropical lower stratosphere. In the middle and upper stratosphere there is a “dipole” of decreases and then increases (Fig. 10a) which are generally less than ±4% of the ozone concentration in Fig. 10b). Note that the “dipole”

Impact of supersaturation

A. Gettelman and
D. E. Kinnison

Title Page

Abstract

Introduction

Conclusions

References

Tables

Figures

◀

▶

◀

▶

Back

Close

Full Screen / Esc

Printer-friendly Version

Interactive Discussion

is also consistent with decreased ozone in the middle stratosphere leading to increased UV penetration and increased ozone at lower levels (a “self-healing” effect). There are several other changes to the chemical balance of the UT/LS region, which occur in the supersaturation simulation and will help with interpreting the changes to ozone. These are discussed briefly below.

Increases in HO_x are expected due to the changes in water vapor in the region. HO_x increases in the supersaturation simulation by 15–20% in the lower tropical stratosphere, located in the same region as the ozone (Fig. 9), temperature (Fig. 4) and water vapor (Fig. 2) increases. Total reactive nitrogen (NO_y) and the more active odd nitrogen molecules ($\text{NO}_x = \text{NO} + \text{NO}_2$) also change in the supersaturation case. The increased HO_x converts more NO_x to HNO_3 , decreasing the NO_x/NO_y ratio between 5–10% (depending on altitude). This has the impact of reducing the odd-oxygen loss importance of NO_y . The opposite is true for the total reactive chlorine (Cl_y) family. Here, increases in HO_x convert more HCl to ClO , and increasing the ClO/HCl ratio by 5–20% (depending on altitude), increasing the odd-oxygen loss importance of the Cl_y family. This chemical sensitivity of increased HO_x repartitioning reservoir species to active forms in the NO_y and Cl_y families is consistent with the discussion in Dvortsov and Solomon (2001).

In line with previous work (Stenke and Grewe, 2005), we see a very small impact of increased H_2O on ozone chemistry in the stratosphere, with impacts of just a few percent above the lower stratosphere. However, it should be pointed out that for a similar (+1 ppmv) perturbation, Stenke and Grewe (2005) reported slight decreases in ozone in the lower-to-mid stratosphere. We see both decreases and increases depending on altitude, latitude, and season. In the UT/LS region, our model is in a situation where there is net ozone production with increased HO_x , leading to a slight increase in ozone in this region (Figs. 9 and 10). An analysis of production and loss rates indicates that the increase in ozone in the UTLS region is likely due to enhanced ozone production through the $\text{HO}_x\text{--NO}_x$ “smog” reactions, as also described by Dvortsov and Solomon (2001). This region of ozone production in the UTLS was not seen by Stenke and

Impact of supersaturation

A. Gettelman and
D. E. Kinnison

Title Page

Abstract

Introduction

Conclusions

References

Tables

Figures

⏪

⏩

◀

▶

Back

Close

Full Screen / Esc

Printer-friendly Version

Interactive Discussion

Grewe (2005). We have compared our ozone loss rates at mid-latitudes where data is available, and find that our odd-oxygen loss processes appear to be adequately represented, i.e., the HO_x and NO_x crossover point is consistent with balloon observations (Osterman et al., 1997). This increases our confidence in our results.

Figure 11 plots the difference in total column ozone between the simulations. Here we see only very small changes in ozone (less than ±3%) outside of the southern hemisphere high latitudes. In the polar southern hemisphere region, ozone decreases are consistent with changes in the temperature and circulation noted above. In this region, temperature decreases (Fig. 4), which increases the heterogeneous conversion on sulfate aerosols of reservoir species (e.g., HCl and ClONO₂) to more active forms (ClO), and increasing odd-oxygen (ozone) loss. The polar southern hemisphere odd-oxygen loss is strongest in austral spring, where it affects column ozone by 10–15% (Fig. 11).

In summary, the changes in ozone are modest, and not significant outside of polar regions. Small ozone increases in the lower stratosphere appear to be due to increases in ozone production via HO_x–NO_x reactions. Above this region, decreases in ozone are consistent with the direct affect of increased catalytic ozone loss from increased HO_x and the affect that increased HO_x has on repartitioning odd-oxygen loss in the NO_y and Cl_y families. The change in ozone in the lower stratosphere is also consistent with the slowing of the mean circulation and with a “self healing” effect of decreasing ozone at upper levels increasing it below.

3.6 Radiation

Changes to the radiation balance of the simulation are expected from the changes to clouds, water vapor and ozone, which together dominate the radiation balance of the UT/LS region, particularly in the Tropical Tropopause Layer (Gettelman et al., 2004). Changes to average tropical heating rates between the two simulations are shown in Fig. 12. These are all sky values (including the effects of clouds). Most of the differences in heating rates between the two simulations occur in the middle and upper

Impact of supersaturation

A. Gettelman and
D. E. Kinnison

Title Page

Abstract

Introduction

Conclusions

References

Tables

Figures

⏪

⏩

◀

▶

Back

Close

Full Screen / Esc

Printer-friendly Version

Interactive Discussion

Impact of supersaturationA. Gettelman and
D. E. Kinnison

[Title Page](#)[Abstract](#)[Introduction](#)[Conclusions](#)[References](#)[Tables](#)[Figures](#)[⏪](#)[⏩](#)[◀](#)[▶](#)[Back](#)[Close](#)[Full Screen / Esc](#)[Printer-friendly Version](#)[Interactive Discussion](#)

5 troposphere. The supersaturation case has slightly lower net heating from the level of zero heating (about 200 hPa) up to 70 hPa, and significantly more cooling in the middle troposphere. Note that is cooling occurs because of more water vapor. This result likely means that there is a complex interplay of the changes to the overlying cloud as well as the direct radiative effects of water vapor. It is also likely that the reduction of cloud cover enhances the clear sky cooling from water vapor throughout this region.

10 In order to investigate the causes of the heating rate differences, we have taken average profiles of temperature, water vapor and cloud liquid water path and input these to an off-line version of the radiative transfer code (a column radiation model). Analysis of these runs indicates that ozone is a negligible contributor to the differences except in the lower stratosphere where the ozone changes modify heating rates by 10–20%. In general, integrating several column runs in latitude yields a global difference in the top of model flux of +0.8 W/m², which is basically the same as the difference in globally averaged residual radiation. The increased absorption due to water vapor in the stratosphere combines with the reduction in cloudiness which allows that water to enter the stratosphere. The moderate impact on lower stratospheric temperatures appears to be due to the radiative effect of clouds, and possible dynamical effects on the residual circulation. We do not see evidence for strong feedbacks of water vapor on tropopause temperatures, particularly the minimum temperatures.

20 4 Discussion and conclusions

4.1 Discussion

Overall, the addition of supersaturation to the WACCM3 coupled chemistry climate model has expected impacts on the simulation of UT/LS humidity and modest further effects on the simulation. In general the model humidity is responding as expected to the imposed changes.

25 The largest humidity effects are decreases in high cloudiness and increases in water

vapor in the stratosphere. The increase is nearly linear with the imposed changes to the condensation closure (about a 20% increase in water vapor). The increase occurs throughout the tropics, and is largest in regions with most cirrus cloudiness (coincident with regions of deep convection in the tropics).

5 In addition to these changes, there appears to be a seasonally varying change in temperature in the tropical tropopause region. This also affects water vapor entering the stratosphere. The largest effects are seen during the “cooling phase” of the annual cycle of tropical tropopause temperatures from August–November. Temperatures during this period are warmer, again throughout much of the tropopause region. It
10 appears as if the cooling is delayed by a month or so in this period, though the final minimum temperatures in January–March at the tropical cold point are similar. This change is an improvement in the base case simulation, which has a smaller annual cycle of tropopause temperatures than observed.

The change in temperature appears to be due to the radiative impacts of reduced
15 high clouds. The shortwave effect appears to dominate over the long wave effect (perhaps counter intuitively). In addition, it appears as if the stratospheric Brewer-Dobson circulation slows in Southern Hemisphere Fall–Winter (August–November), from an analysis of the TEM residual circulation, long lived tracers and Age of Air estimates. The circulation changes are coherent with the temperature changes. The age of air
20 increases by about 10–20% in Southern Hemisphere high latitudes. These changes are largest in the August–November period.

The chemical impact of the changes is modest in the tropics and more significant at high latitudes. We see very little impact on tropical column ozone. There are small increases in ozone in the lower stratosphere, which appear to be due to increased
25 production via HO_x – NO_x “smog” reactions. The changes are also consistent with a slowing of the circulation.

In high latitudes, the changes to the tropical temperatures and resultant change in the circulation significantly affect Southern Hemisphere polar ozone. Decreases in temperature in August–November increase ozone loss reactions, resulting in column

Impact of supersaturation

A. Gettelman and
D. E. Kinnison

[Title Page](#)[Abstract](#)[Introduction](#)[Conclusions](#)[References](#)[Tables](#)[Figures](#)[⏪](#)[⏩](#)[◀](#)[▶](#)[Back](#)[Close](#)[Full Screen / Esc](#)[Printer-friendly Version](#)[Interactive Discussion](#)

decreases of 10–15%.

We have looked in detail at the heating rates in the tropics, and the increases in ozone do not appear to be affecting the heating rates. Since the amplitude of the annual cycle of tropical tropopause temperatures is too small in the base case, and summer-time water vapor slightly low, the changes with supersaturation represent an improvement to the mean model climate. These changes ultimately are forced by changes to tropical cloudiness as noted above.

Since the simulations use fixed surface temperatures, these simulations are not designed to examine effects of stratospheric water vapor on surface temperatures. We also do not see evidence of a strong “stratospheric water vapor feedback” (Stuber et al., 2001) in the simulations from changing stratospheric water vapor by 10–20%. The UT/LS region may be more sensitive to radiative forcing, but the coupled chemistry and physics limit the impact. In this work, with an internally consistent method for a modest change in water vapor, we note a top of atmosphere change in the radiative balance of $+0.8 \text{ Wm}^{-2}$. This is not the direct effect of the increase in stratospheric water vapor, because it also includes the effect of significant modifications to clouds, and the reduction in net cloud forcing (which is negative, so the change is positive) of $+0.6 \text{ Wm}^{-2}$, which contributes the largest share to the change in radiative balance in the model. The residual of about $+0.2 \text{ Wm}^{-2}$ is similar to that found by Forster and Shine (2002) for a similar change in stratospheric water vapor. Thus in these simulations clouds are the dominant response, but stratospheric water vapor appears to respond as found in previous work. In general, if changes to stratospheric water vapor were coupled to significant changes in cloudiness in the tropopause region, the cloud radiative effects would likely swamp any direct radiative impact of stratospheric water vapor.

4.2 Implications for global models

This study has several important implications for global model treatments of the UT/LS region. First is that stratospheric water vapor responds directly to temperature changes

Impact of supersaturation

A. Gettelman and
D. E. Kinnison

Title Page

Abstract

Introduction

Conclusions

References

Tables

Figures

◀

▶

◀

▶

Back

Close

Full Screen / Esc

Printer-friendly Version

Interactive Discussion

in WACCM3. Thus getting appropriate temperature variability on seasonal to annual and inter-annual timescales is important for the future trajectory of the stratosphere. It is however difficult to know what the expected trend in tropical tropopause temperatures is. We know that changes to water vapor in the stratosphere are expected from oxidation of methane (SPARC, 2000) and that these changes are not monotonic trends (Randel et al., 2004).

It is clear from the simulations that stratospheric water vapor responds to temperatures. It is also clear that changes to the threshold for condensation can have significant impacts on clouds. The radiative effects of these clouds can have significant effects on the coupled chemistry and climate of the stratosphere. In these simulations, enhanced upwelling radiation and possibly increased water vapor, may be affecting tropical lower stratospheric temperatures, and by reducing the overturning Brewer-Dobson circulation, this appears to enhance polar ozone loss. This implies that changes to the distribution of aerosols that are ice nuclei which modify supersaturation may be important for affecting tropical clouds, stratospheric water vapor and even polar ozone. However, this result is likely to be dependent on the WACCM model biases, seasonality of effects on clouds and particularly an existing cold pole bias. Actual impacts on polar ozone are likely more modest.

The weakening of the stratospheric circulation found in these simulations runs counter to the strengthening of the circulation found for many of the models (including WACCM) forced with greenhouse gases by Butchart et al. (2006). The runs in Butchart et al. (2006) should have included some increases of water vapor due to increases in methane. But the water vapor changes in the Butchart et al. (2006) simulations would have a different distribution (peaking in the upper stratosphere) than presented here (peaking in the lower stratosphere), which combined with the significant changes to clouds likely is the cause of the different response. This highlights however an additional uncertainty in predicting the future state of the stratosphere.

Finally, we restate that this is a very crude way to implement supersaturation, but one that is consistent with the model physics. This study was intended as a scoping exer-

Impact of supersaturationA. Gettelman and
D. E. Kinnison

Title Page

Abstract

Introduction

Conclusions

References

Tables

Figures

◀

▶

◀

▶

Back

Close

Full Screen / Esc

Printer-friendly Version

Interactive Discussion

cise, where we impose a change consistent with the model framework and investigate the impact of the change on the coupled system. In general, the supersaturation case has a better representation of water vapor in the stratosphere due to improvements in the annual cycle of tropical tropopause temperatures, but excessive ozone loss and an enhanced cold pole problem in the Southern hemisphere polar region.

Treatments for global models using these ideas for cold (ice) clouds exist (Kärcher et al., 2006). And better treatments for cloud closures in global models that allow bulk supersaturation have also been developed (Tompkins et al., 2006). This study highlights the importance of using these more realistic treatments for supersaturation in future global models.

Acknowledgements. Thanks to S. Walters for assistance with WACCM runs and acerbic encouragement. We also thank J. F. Lamarque, F. Sassi and W. J. Randel for comments. The National Center for Atmospheric Research is supported by the United States National Science Foundation.

References

- Andrews, D., Holton, J., and Leovy, C.: Middle Atmosphere Dynamics, Academic Press, New York, 1987. [12444](#)
- Boville, B. A., Rasch, P. J., Hack, J. J., and McCaa, J. R.: Representation of Clouds and Precipitation in the Community Atmosphere Model Version 3 (CAM3), *J. Climate*, 19, 2184–2198, 2006. [12438](#)
- Brasseur, G. P., Hauglustaine, D. A., Walters, S., Rasch, P. J., Muller, J.-F., Granier, C., and Tie, X. X.: MOZART, a global chemical transport model for ozone and related chemical tracers 1. Model description, *J. Geophys. Res.*, 103, 28 265–28 289, 1998. [12437](#)
- Butchart, N., Scaife, A. A., Bourqui, M., et al.: A multi-model study of climate change in the Brewer-Dobson circulation, in press, *Clim. Dyn.*, 27(7–8), 727–741, doi:10.1007/s00382-006-0162-4, 2006. [12452](#)
- Cess, R. D.: Water Vapor Feedback in Climate Models, *Science*, 310, 795–796, 2005. [12435](#)
- Collins, W. D., Rasch, P. J., Boville, B. A., Hack, J. J., McCaa, J. R., Williamson, D. L., Briegleb,

Impact of supersaturation

A. Gettelman and
D. E. Kinnison

Title Page

Abstract

Introduction

Conclusions

References

Tables

Figures

◀

▶

◀

▶

Back

Close

Full Screen / Esc

Printer-friendly Version

Interactive Discussion

- B. P., Bitz, C. M., Lin, S.-J., and Zhang, M.: The Formulation and Atmospheric Simulation of the Community Atmosphere Model: CAM3, *J. Climate*, 19, 2122–2161, 2006. [12437](#)
- Dvortsov, V. L. and Solomon, S.: Response of the stratospheric temperatures and ozone to past and future increases in stratospheric humidity, *J. Geophys. Res.*, 106, 7505–7514, 2001. [12447](#)
- 5 Eyring, V., Butchart, N., Waugh, D. W., et al.: Assessment of coupled chemistry-climate models: Evaluation of dynamics, transport and ozone, *J. Geophys. Res.*, 111, D22308, doi:10.1029/2006JD007327, 2006.
- Forster, P. M. d. F. and Shine, K. P.: Assessing the climate impact of trends in stratospheric water vapor, *Geophys. Res. Lett.*, 29, 1086, doi:10.1029/2001GL013909, 2002. [12436](#), [12439](#), [12451](#)
- 10 Gettelman, A., Forster, P. M. F., Fujuwara, M., Fu, Q., Vomel, H., Gohar, L. K., Johanson, C., and Ammeraman, M.: The Radiation Balance of the Tropical Tropopause Layer, *J. Geophys. Res.*, 109, D07103, doi:10.1029/2003JD004190, 2004. [12448](#)
- 15 Gettelman, A., Fetzer, E. J., Irion, F. W., and Eldering, A.: The Global Distribution of Supersaturation in the Upper Troposphere, *J. Climate*, 19(23), 6089–6103, 2006. [12435](#), [12436](#)
- Gierens, K. and Spichtinger, P.: On the size distribution of ice supersaturation regions in the upper troposphere and lower stratosphere, *Ann. Geophys.*, 18, 499–504, 2000, <http://www.ann-geophys.net/18/499/2000/>. [12436](#)
- 20 Holton, J. R. and Gettelman, A.: Horizontal transport and dehydration in the stratosphere, *Geophys. Res. Lett.*, 28, 2799–2802, 2001. [12435](#)
- Holton, J. R., Haynes, P. H., Douglass, A. R., Rood, R. B., and Pfister, L.: Stratosphere–Troposphere Exchange, *Rev. Geophys.*, 33, 403–439, 1995. [12442](#)
- Horowitz, L. W., Walters, S., Mauzerall, D. L., et al.: A global simulation of tropospheric ozone and related tracers: Description and Evaluation of MOZART, version 2, *J. Geophys. Res.*, 25 108(D4), 4784, doi:10.1029/2002JD002853, 2003. [12437](#)
- Jensen, E., Smith, J. B., Pfister, L., et al.: Ice Supersaturations exceeding 100% at the cold tropical tropopause: implications for cirrus formation and dehydration, *Atmos. Chem. Phys.*, 5, 851–862, 2005, <http://www.atmos-chem-phys.net/5/851/2005/>. [12435](#)
- 30 Jensen, E. J., Read, W. G., Mergenthaler, J., Sandor, B. J., Pfister, L., and Tabazadeh, A.: High humidities and subvisible cirrus near the tropical tropopause, *Geophys. Res. Lett.*, 26, 2347–2350, 1999. [12435](#)
- Joshi, M., Shine, K., Ponater, M., Stuber, N., Sausen, R., and Li, L.: A comparison of climate

Impact of supersaturationA. Gettelman and
D. E. Kinnison

Title Page

Abstract

Introduction

Conclusions

References

Tables

Figures

◀

▶

◀

▶

Back

Close

Full Screen / Esc

Printer-friendly Version

Interactive Discussion

Impact of supersaturationA. Gettelman and
D. E. Kinnison

Title Page

Abstract

Introduction

Conclusions

References

Tables

Figures

◀

▶

◀

▶

Back

Close

Full Screen / Esc

Printer-friendly Version

Interactive Discussion

response to different radiative forcings in three general circulation models: towards an improved metric of climate change, *Clim. Dyn.*, 20, 843–854, doi:10.1007/s00382-003-0305-9, 2003. [12436](#)

5 Kärcher, B. and Haag, W.: Factors controlling upper tropospheric relative humidity, *Ann. Geophys.*, 22, 705–715, 2004, <http://www.ann-geophys.net/22/705/2004/>. [12435](#)

Kärcher, B. and Lohmann, U.: A parameterization of cirrus cloud formation: Homogenous freezing of supercooled aerosols, *J. Geophys. Res.*, 107, 4010, doi:10.1029/2001JD000470, 2002a. [12436](#), [12439](#)

10 Kärcher, B. and Lohmann, U.: A parameterization of cirrus cloud formation: Homogenous freezing including effects of aerosol size, *J. Geophys. Res.*, 107, 4698, doi:10.1029/2001JD001429, 2002b. [12436](#)

Kärcher, B., Hendricks, J., and Lohmann, U.: Physically based parameterization of cirrus cloud formation for use in atmospheric models, *J. Geophys. Res.*, 111, D01205, doi:10.1029/2005JD006219, 2006. [12436](#), [12453](#)

15 Koop, T., Luo, B., Tsias, A., and Peter, T.: Water activity as the determinant for homogenous ice nucleation in aqueous solutions, *Nature*, 406, 611–614, 2000. [12435](#)

Mote, P. W., Rosenlof, K. H., McIntyre, M. E., et al.: An atmospheric tape recorder: The imprint of tropical tropopause temperatures on stratospheric water vapor, *J. Geophys. Res.*, 101, 3989–4006, 1996. [12442](#)

20 Murphy, D. M. and Koop, T.: Review of the vapour pressure of ice and supercooled water for atmospheric applications, *Q. J. R. Meteorol. Soc.*, 131, 1539–1565, 2005. [12434](#)

Osterman, G. B., Salawitch, R. J., Sen, B., Toon, G. C., Stachnik, R. A., Pickett, H. M., Margitan, J. J., Blavier, J. F., and Peterson, D. B.: Balloon-borne measurements of stratospheric radicals and their precursors: Implications for the production and loss of ozone, *Geophys. Res. Lett.*, 24, 1107–1110, 1997. [12448](#)

25 Ramanathan, V., Cess, R. D., Harrison, E. F., Minnis, P., Barkstrom, B. R., Ahmad, E., and Hartmann, D.: Cloud-Radiative Forcing and Climate: Results from the Earth Radiation Budget Experiment, *Science*, 243, 57–63, 1989. [12441](#)

30 Randel, W. J., Gettelman, A., Wu, F., Russell III, J. M., Zawodny, J., and Oltmans, S.: Seasonal variation of water vapor in the lower stratosphere observed in Halogen Occultation Experiment data, *J. Geophys. Res.*, 106, 14 313–14 325, 2001. [12442](#)

Randel, W. J., Wu, F., Oltmans, S. J., Rosenlof, K., and Nedoluha, G. E.: Interannual changes of

- stratospheric water vapor and correlations with tropical tropopause temperatures, *J. Atmos. Sci.*, 61, 2133–2148, 2004. [12452](#)
- Rasch, P. J. and Kristjansson, J. E.: A Comparison of CCM3 Model climate using diagnosed and predicted condensate parameterizations, *J. Climate*, 11, 1587–1614, 1998. [12436](#), [12438](#)
- Slingo, J. M.: The development and verification of a cloud prediction scheme for the ECMWF model, *Q. J. R. Meteorol. Soc.*, 113, 899–927, 1987. [12438](#)
- SPARC: Assessment of Water Vapor in the Upper Troposphere and Lower Stratosphere, WMO/TD-1043, Stratospheric Processes and Their Role In Climate, World Meteorological Organization, Paris, 2000. [12442](#), [12452](#)
- Spichtinger, P., Gierens, K., Leiterer, U., and Dier, H.: Ice supersaturation in the tropopause region over Lindenberg, Germany, *Meteorologische Zeitschrift*, 12, 143–156, 2003a. [12435](#)
- Spichtinger, P., Gierens, K., and Read, W.: The global distribution of ice-supersaturated regions as seen by the Microwave Limb Sounder, *Q. J. R. Meteorol. Soc.*, 129, 3391–3410, 2003b. [12435](#)
- Stenke, A. and Grewe, V.: Simulation of stratospheric water vapor trends: impact on stratospheric ozone chemistry, *Atmos. Chem. Phys.*, 5, 1257–1272, 2005, <http://www.atmos-chem-phys.net/5/1257/2005/>. [12439](#), [12447](#)
- Stuber, N., Ponater, M., and Sausen, R.: Is the climate sensitivity to ozone perturbations enhanced by stratospheric water vapor feedback?, *Geophys. Res. Lett.*, 28, 2887–2890, 2001. [12436](#), [12451](#)
- Stuber, N., Ponater, M., and Sausen, R.: Why radiative forcing might fail as a predictor of climate change, *Clim. Dyn.*, 24, 497–510, doi:10.1007/s00382-004-0497-7, 2005. [12436](#), [12439](#)
- Tompkins, A. M., Gierens, K., and Rädcl, G.: Ice supersaturation in the ECMWF forecast system,, *Quart. J. Royal Meteorol. Soc.*, in press, 2006. [12453](#)
- Waugh, D. W. and Hall, T. M.: Age of Stratospheric Air: Theory, Observations and Models, *Rev. Geophys.*, 40, 2002. [12445](#)
- Wennberg, P. O., Cohen, R. C., Stimpfle, R. M., Koplów, J. P., Anderson, J. G., Salawitch, R. J., Fahey, D. W., Woodbridge, E. L., Keim, E. R., Gao, R. S., Webster, C. R., May, R. D., Toohey, D. W., Avallone, L. M., Proffitt, M. H., Loewenstein, M., Podolske, J. R., Chan, K. R., and Wofsy, S. C.: Removal of Stratospheric O₃ by Radicals: In Situ Measurements of OH, HO₂, NO, NO₂, ClO and BrO, *Science*, 266, 398–404, 1994. [12435](#)

Impact of supersaturation

A. Gettelman and
D. E. Kinnison

[Title Page](#)[Abstract](#)[Introduction](#)[Conclusions](#)[References](#)[Tables](#)[Figures](#)[◀](#)[▶](#)[◀](#)[▶](#)[Back](#)[Close](#)[Full Screen / Esc](#)[Printer-friendly Version](#)[Interactive Discussion](#)

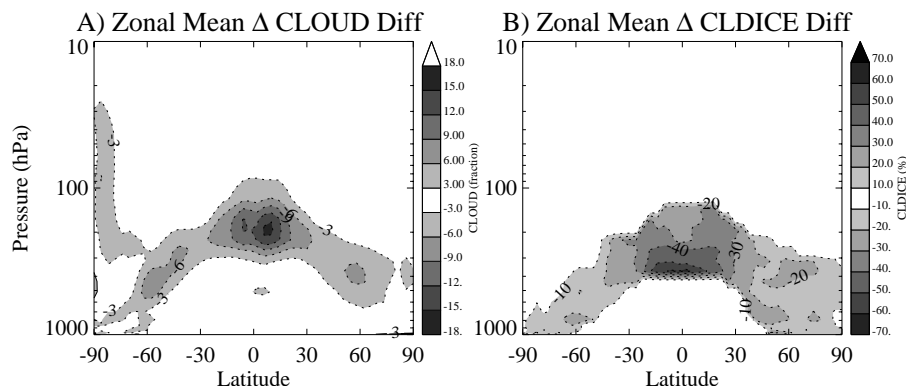
Impact of supersaturationA. Gettelman and
D. E. Kinnison

Fig. 1. Annual zonal mean differences (Supersaturation – Base) in **(a)** cloud fraction and **(b)** cloud ice water mixing ratio.

[Title Page](#)[Abstract](#)[Introduction](#)[Conclusions](#)[References](#)[Tables](#)[Figures](#)[◀](#)[▶](#)[◀](#)[▶](#)[Back](#)[Close](#)[Full Screen / Esc](#)[Printer-friendly Version](#)[Interactive Discussion](#)

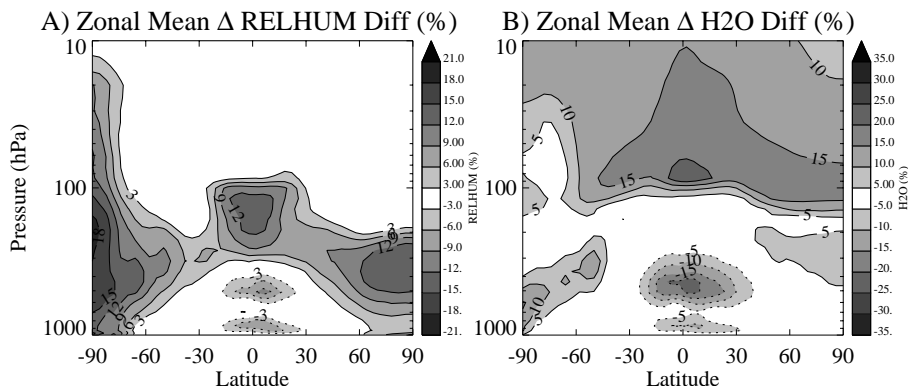
Impact of
supersaturationA. Gettelman and
D. E. Kinnison

Fig. 2. Annual zonal mean differences (Supersaturation – Base) in **(a)** Relative Humidity and **(b)** water vapor (specific humidity) mixing ratio.

[Title Page](#)[Abstract](#)[Introduction](#)[Conclusions](#)[References](#)[Tables](#)[Figures](#)[◀](#)[▶](#)[◀](#)[▶](#)[Back](#)[Close](#)[Full Screen / Esc](#)[Printer-friendly Version](#)[Interactive Discussion](#)

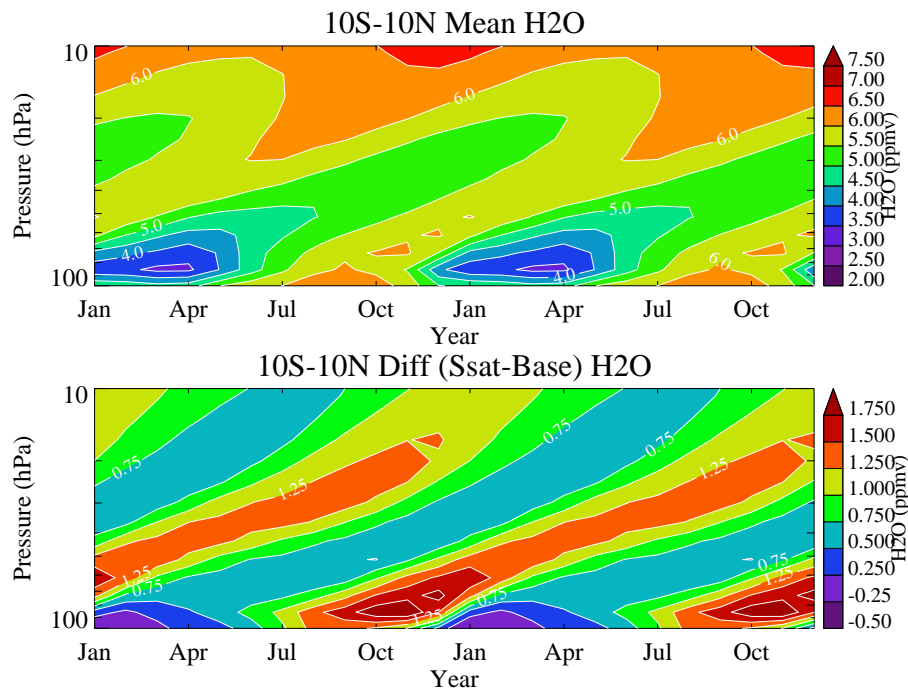
Impact of
supersaturationA. Gettelman and
D. E. Kinnison

Fig. 3. Zonal mean tropical (10S–10N) monthly water vapor on the equator for (a) Base case (Top) and (b) difference between supersaturation and base cases (SSAT – Base) in ppmv (bottom). Mean annual cycle is repeated twice.

[Title Page](#)[Abstract](#)[Introduction](#)[Conclusions](#)[References](#)[Tables](#)[Figures](#)[◀](#)[▶](#)[◀](#)[▶](#)[Back](#)[Close](#)[Full Screen / Esc](#)[Printer-friendly Version](#)[Interactive Discussion](#)

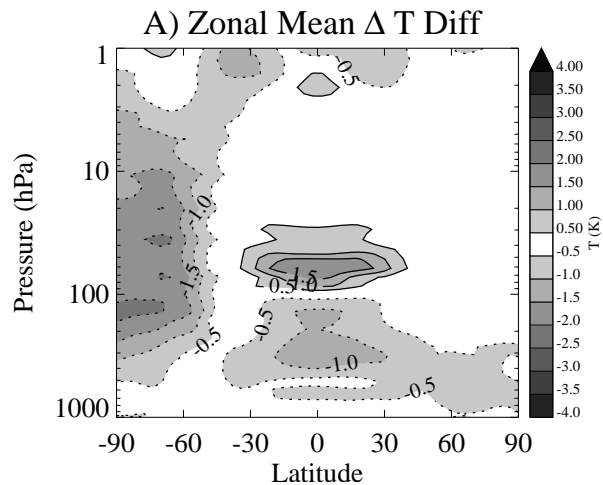
**Impact of
supersaturation**A. Gettelman and
D. E. Kinnison

Fig. 4. Annual zonal mean differences (Supersaturation – Base) in Temperature in °K.

Title Page

Abstract

Introduction

Conclusions

References

Tables

Figures

◀

▶

◀

▶

Back

Close

Full Screen / Esc

Printer-friendly Version

Interactive Discussion

Impact of supersaturation

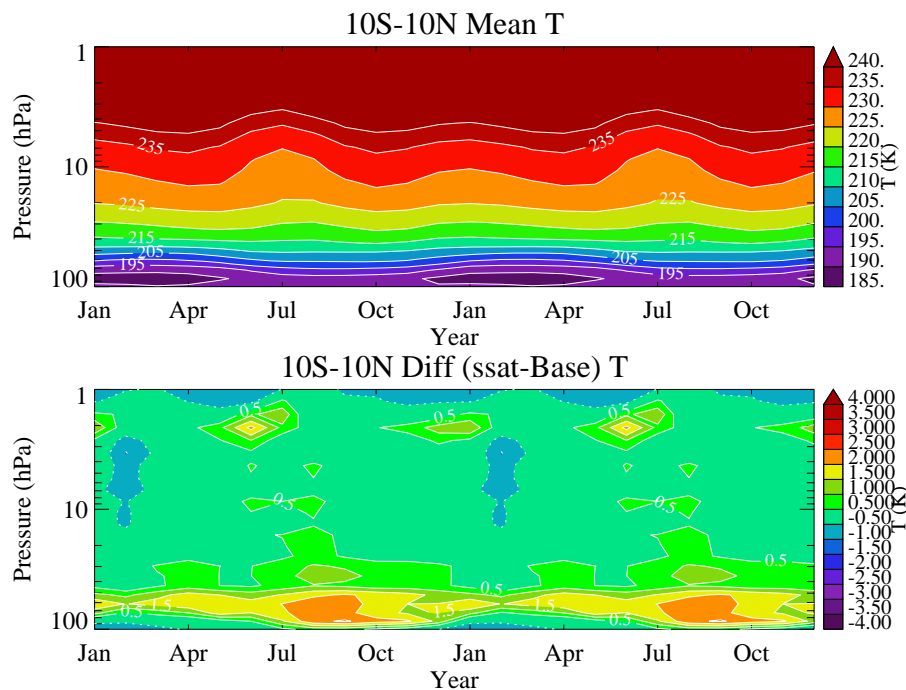
A. Gettelman and
D. E. Kinnison

Fig. 5. Zonal mean tropical (10S–10N) monthly temperature (in °K) on the equator for **(a)** Base case (Top) and **(b)** difference between supersaturation and base cases (SSAT – Base) (bottom). Mean annual cycle is repeated twice.

Title Page

Abstract

Introduction

Conclusions

References

Tables

Figures

◀

▶

◀

▶

Back

Close

Full Screen / Esc

Printer-friendly Version

Interactive Discussion

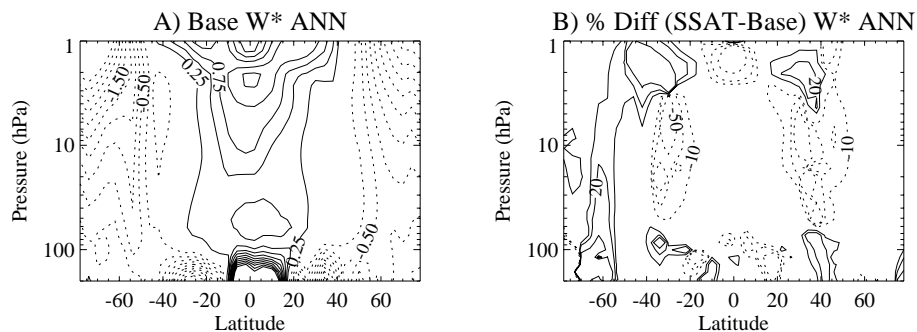
Impact of supersaturationA. Gettelman and
D. E. Kinnison

Fig. 6. Annual mean residual vertical velocity (\bar{w}^*) in cm/s A) base case. Contour interval 0.25 cm/s. B) Percent difference between supersaturation and base case (ssat – base). Contour interval ± 10 , 20 and 50%.

[Title Page](#)[Abstract](#)[Introduction](#)[Conclusions](#)[References](#)[Tables](#)[Figures](#)[◀](#)[▶](#)[◀](#)[▶](#)[Back](#)[Close](#)[Full Screen / Esc](#)[Printer-friendly Version](#)[Interactive Discussion](#)

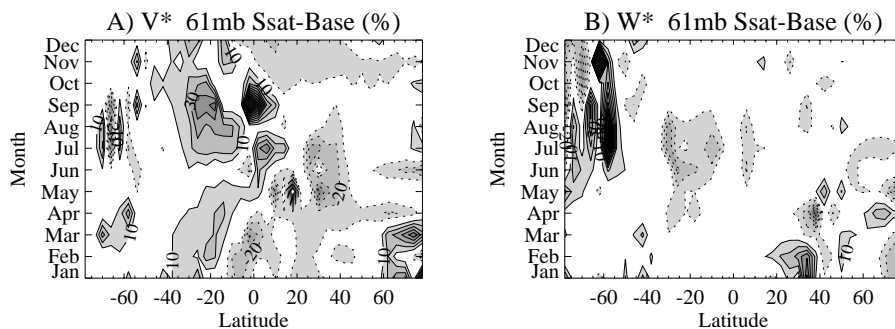
Impact of supersaturationA. Gettelman and
D. E. Kinnison

Fig. 7. Annual cycle of monthly mean differences (Supersaturation – Base) in percent for **(a)** TEM meridional residual velocity (v^*) and **(b)** TEM vertical residual velocity (w^*).

Title Page

Abstract

Introduction

Conclusions

References

Tables

Figures

◀

▶

◀

▶

Back

Close

Full Screen / Esc

Printer-friendly Version

Interactive Discussion

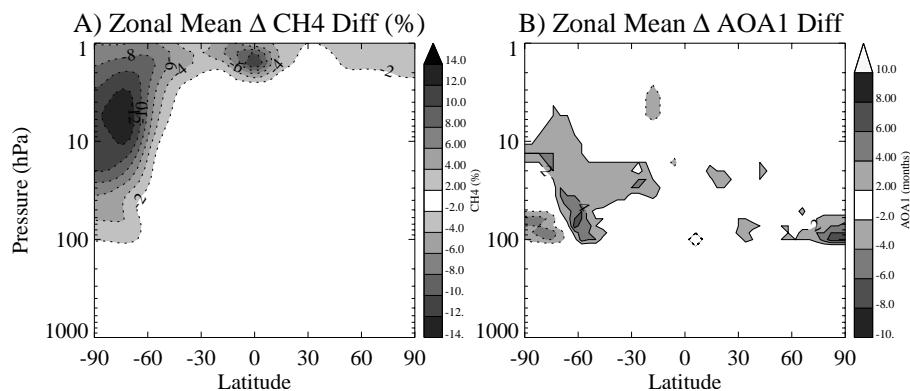
Impact of supersaturationA. Gettelman and
D. E. Kinnison

Fig. 8. Annual zonal mean differences (Supersaturation – Base) in **(a)** CH₄ mixing ratio (%) and **(b)** Difference in Age of Air (AOA) in Months.

[Title Page](#)[Abstract](#)[Introduction](#)[Conclusions](#)[References](#)[Tables](#)[Figures](#)[◀](#)[▶](#)[◀](#)[▶](#)[Back](#)[Close](#)[Full Screen / Esc](#)[Printer-friendly Version](#)[Interactive Discussion](#)

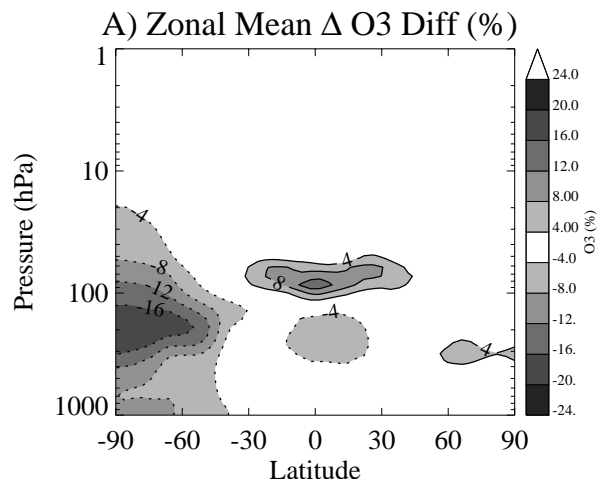
Impact of supersaturationA. Gettelman and
D. E. Kinnison

Fig. 9. Annual zonal mean percent differences (Supersaturation – Base) in Ozone mixing ratio.

Title Page

Abstract

Introduction

Conclusions

References

Tables

Figures

◀

▶

◀

▶

Back

Close

Full Screen / Esc

Printer-friendly Version

Interactive Discussion

Impact of supersaturation

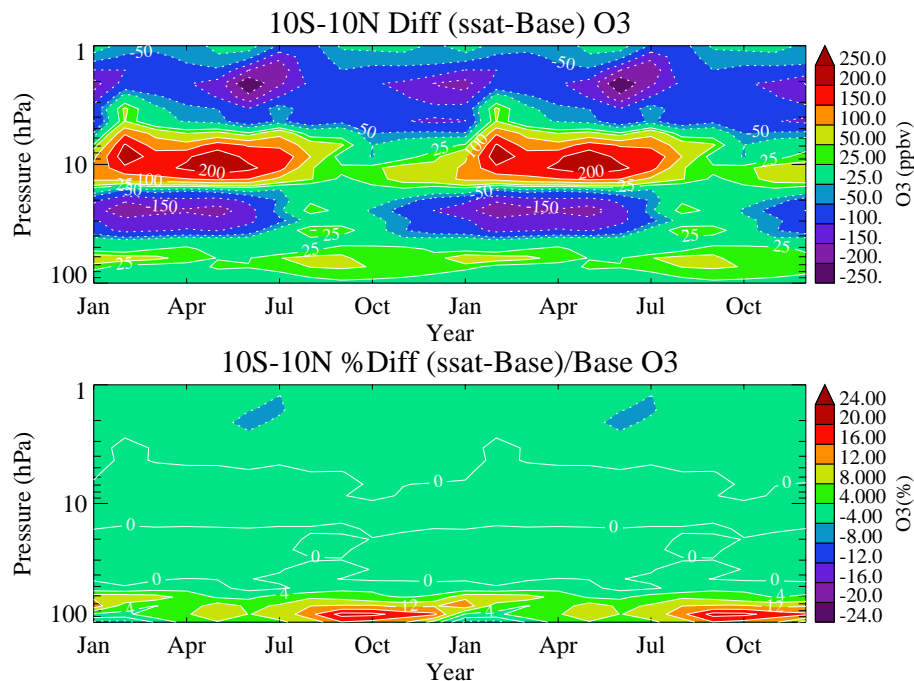
A. Gettelman and
D. E. Kinnison

Fig. 10. Zonal mean tropical (10S–10N) monthly ozone difference between supersaturation and base cases. **(a)** Top: difference (in ppbv) and **(b)** bottom: percent difference (SSAT – Base)/Base. Mean annual cycle is repeated twice. Contour levels in top panel are not regular.

Title Page

Abstract

Introduction

Conclusions

References

Tables

Figures

◀

▶

◀

▶

Back

Close

Full Screen / Esc

Printer-friendly Version

Interactive Discussion

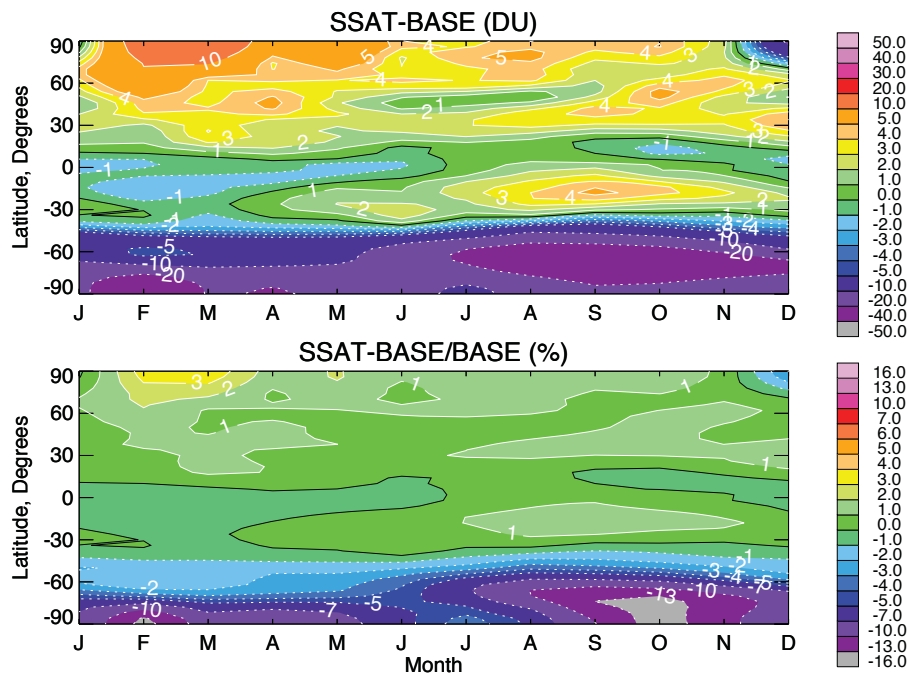
Impact of supersaturationA. Gettelman and
D. E. Kinnison

Fig. 11. Zonal mean Column ozone monthly difference between supersaturation and base cases. **(a)** Top: difference (in DU) and **(b)** bottom: percent difference $(SSAT - Base)/Base$.

Title Page

Abstract

Introduction

Conclusions

References

Tables

Figures

◀

▶

◀

▶

Back

Close

Full Screen / Esc

Printer-friendly Version

Interactive Discussion

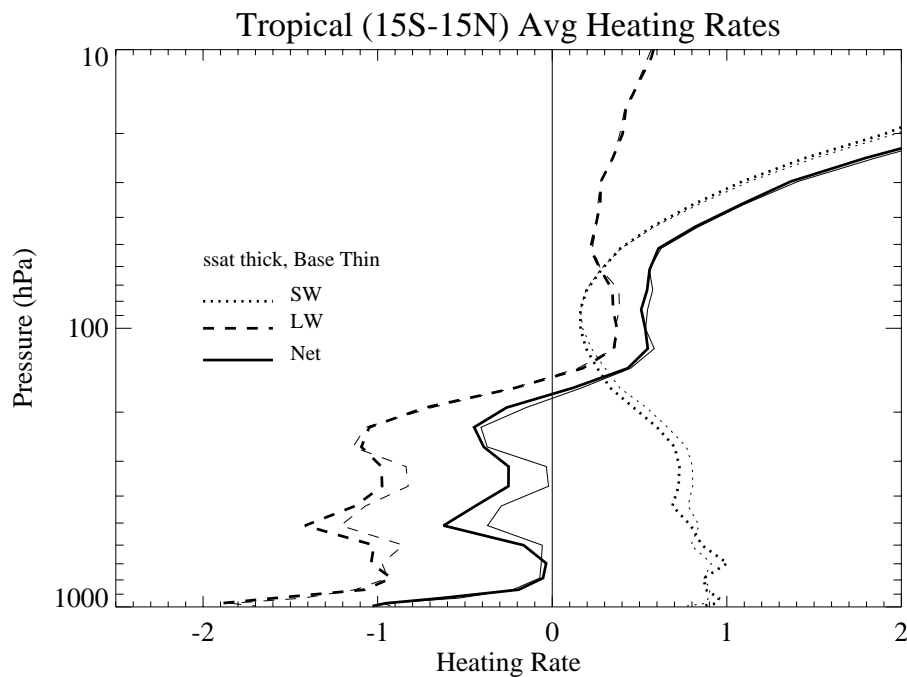
Impact of supersaturationA. Gettelman and
D. E. Kinnison

Fig. 12. Mean tropical (15 S–15 N) average heating rates (in K day^{-1}) for the Base case (thin) and Supersaturated case (thick). Net radiation solid, longwave dashed, shortwave dotted.

[Title Page](#)[Abstract](#)[Introduction](#)[Conclusions](#)[References](#)[Tables](#)[Figures](#)[◀](#)[▶](#)[◀](#)[▶](#)[Back](#)[Close](#)[Full Screen / Esc](#)[Printer-friendly Version](#)[Interactive Discussion](#)